哈爾濱工業大學(深圳) Harbin Institute of Technology, Shenzhen
湍流-噪声-振动耦合与控制研究所
Institute for Turbulence-Noise-Vibration Interactions and Control

Artificial intelligence control of turbulence

Yu Zhou

with D W Fan, B Noack, R Li, Z Wu

ACKNOWLEDGEMENTS

This work was supported from NSFC through grants 11632006 and 91752109.

5th Symposium on Fluid-Structure-Sound Interactions and Control, Chania, 27th - 30th August 2019

OUTLINE

1. Motivation
2. Artificial intelligence control system
3. Presentation of results on jet manipulation
4. Conclusions & outlook

Motivation

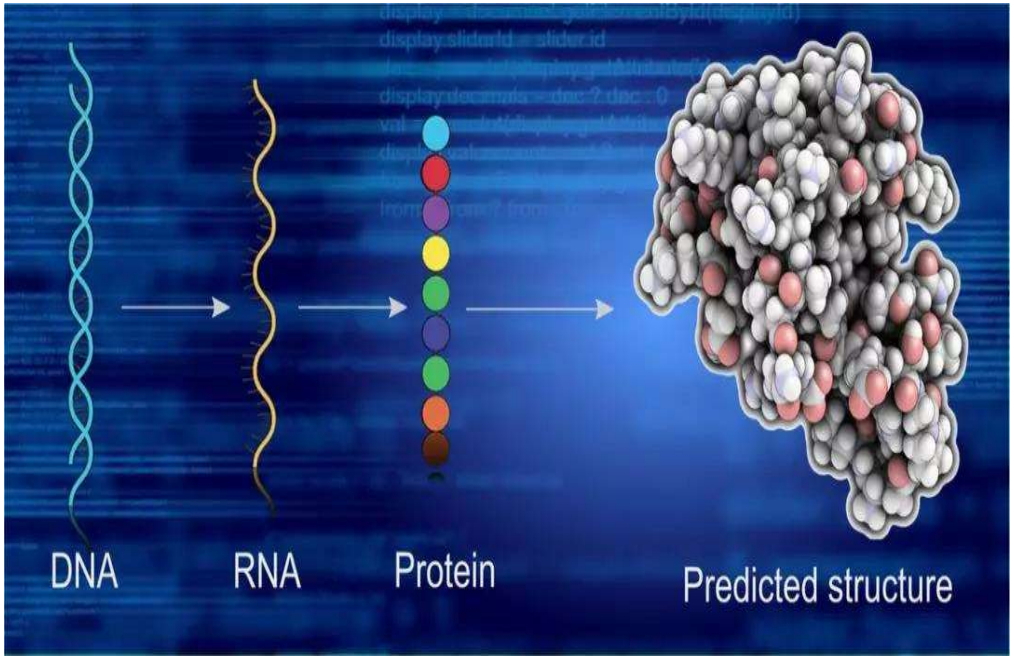

AlphaGo **AlphaFold**

Human beings have so far been the most intelligent species on the earth in the past 100,000 years evolution. However, it seems that we are facing the fact that a more intelligent species is emerging, i.e. artificial intelligence (AI). One big question is: could we take the advantage of AI for turbulence control?

Objective

This talk aims to illustrate the potential of artificial intelligence in turbulence control.

AI control system for turbulent jet mixing enahncement

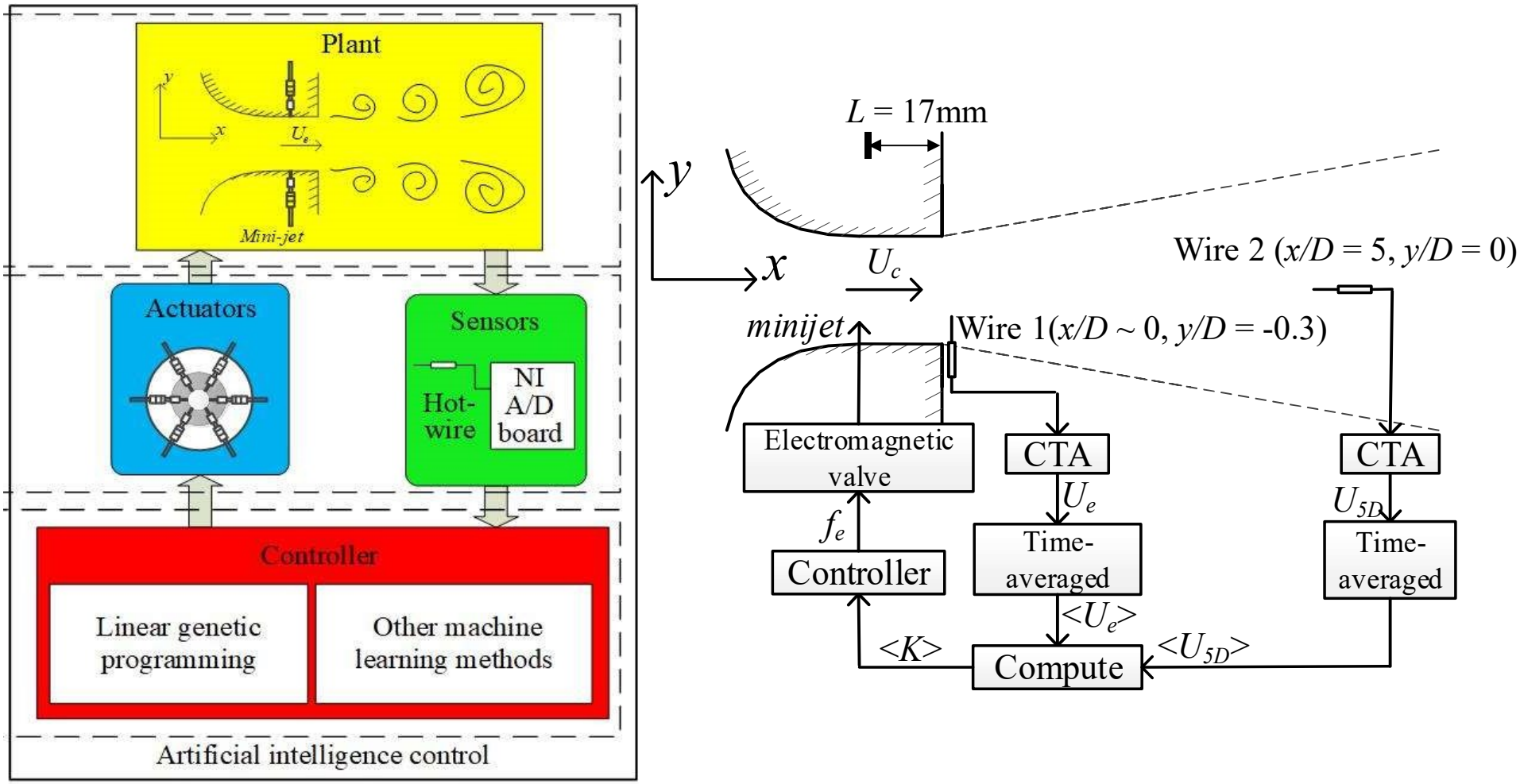

Artificial intelligence control (AIC) system which consists of sensors (green), a controller (red) that includes linear genetic programming (LGP) algorithm, memorizing, and decision-making elements, actuators (blue) and plant (yellow).

Experimental set-up

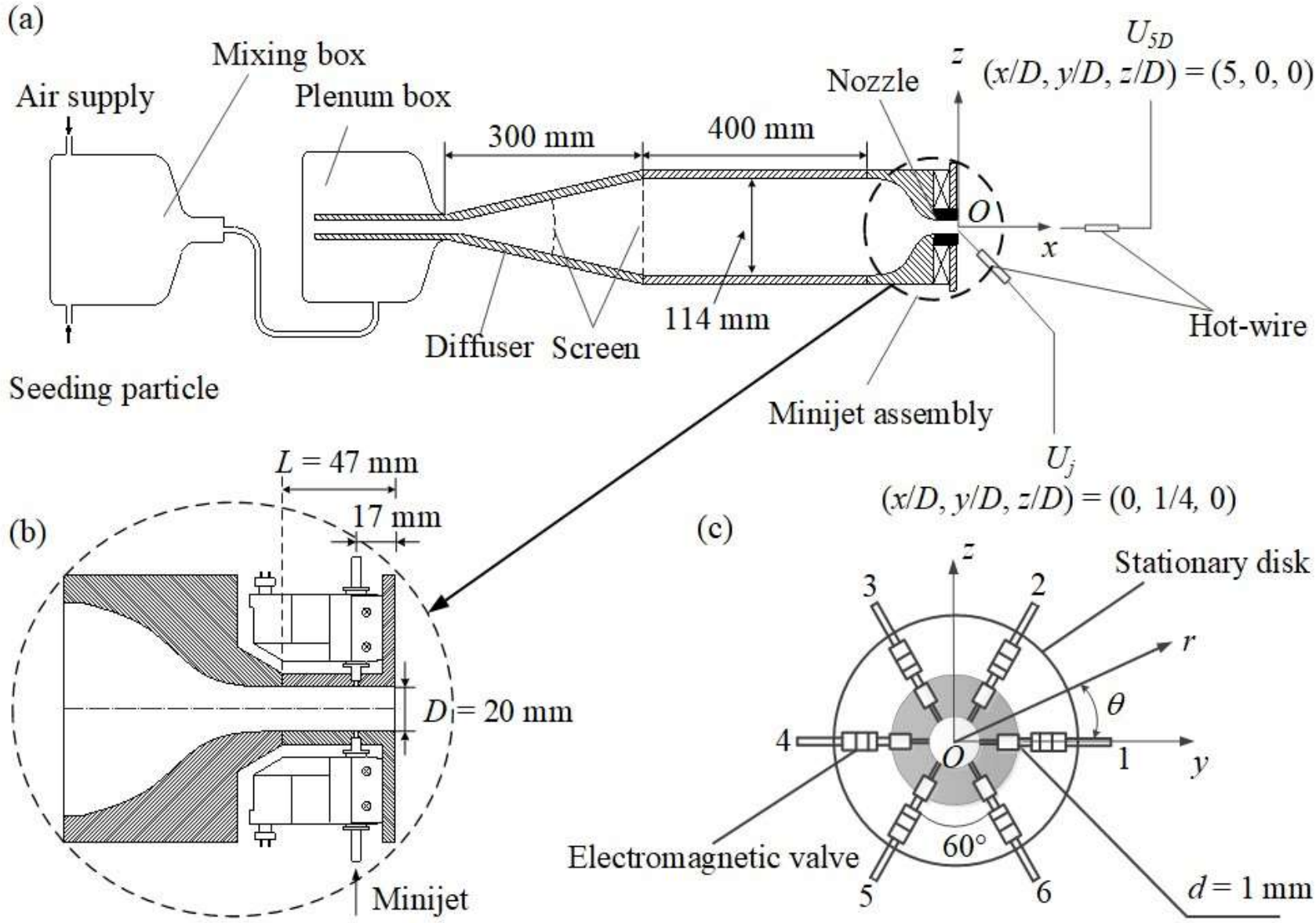

Control plant, actuator and sensor

Control parameters involved with multiple independent minijets

Control parameters

- **Minijet number** — N
- **Ratio of the minijet frequency to the preferred-mode frequency of the main jet** — f_e/f_0
- **Mass flow rate ratio of each minijet to the main jet** — C_m
- **Duty cycle of unsteady minijets** — α_i
- **Temporal phase shift between minijets** — $\varphi_{i,j}$
- **Spatial separation angle between minijets** — $\theta_{i,j}$

(*i*, *j* = 1, 2, …, 6)

Jet entrainment/ mixing evaluation

Jet centerline mean velocity decay rate (Perumal & Zhou 2018 JFM)

$$K = \frac{U_e - U_{x/D=5}}{U_e}$$

$$K = K\ (N,\ \theta_{i,j},\ \varphi_{i,j},\ f_e/f_0,\ C_m,\ \alpha_i,\ \ldots)$$

The key question:
How to find the global optimal solution of
$K = K(N, \theta_{i,j}, \varphi_{i,j}, f_e/f_0, C_m, \alpha_i)$ **?**

Conventional open-loop control

Jet mixing dependence on f_e/f_0 and C_m (α = 14.5%)

Minijet configurations

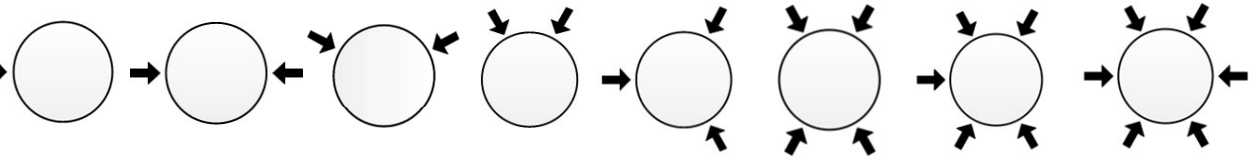

$K = K(f_e/f_0)$

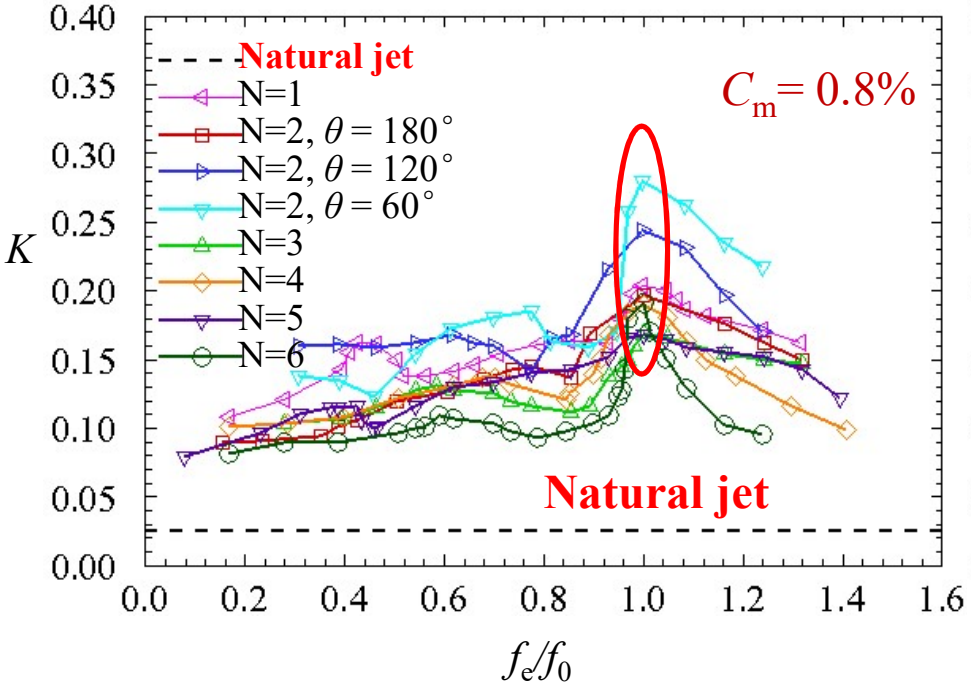

$K = K(C_m)$

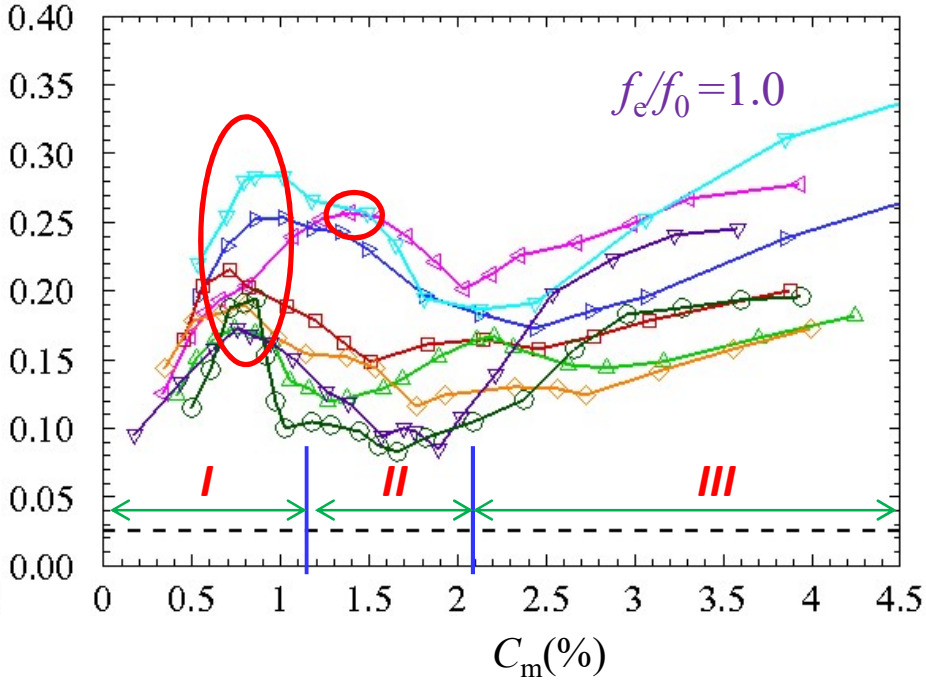

Yang et al. (2016, RSPA), Yang & Zhou (2016, JFM)

Flow structure for $N = 1$

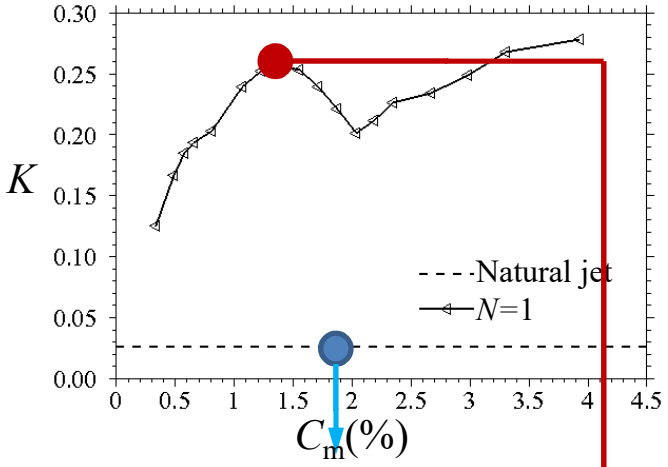

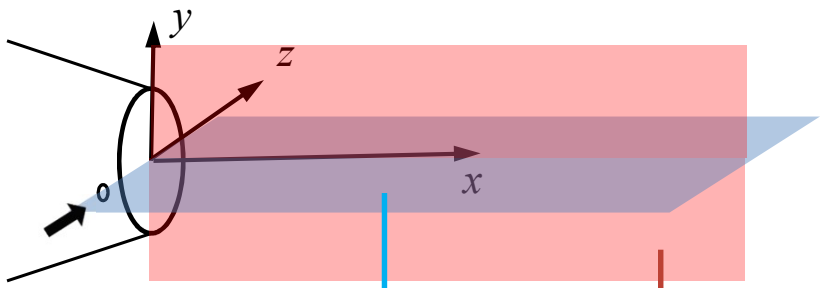

Injection plane

Non-injection plane

Wobbling left and right

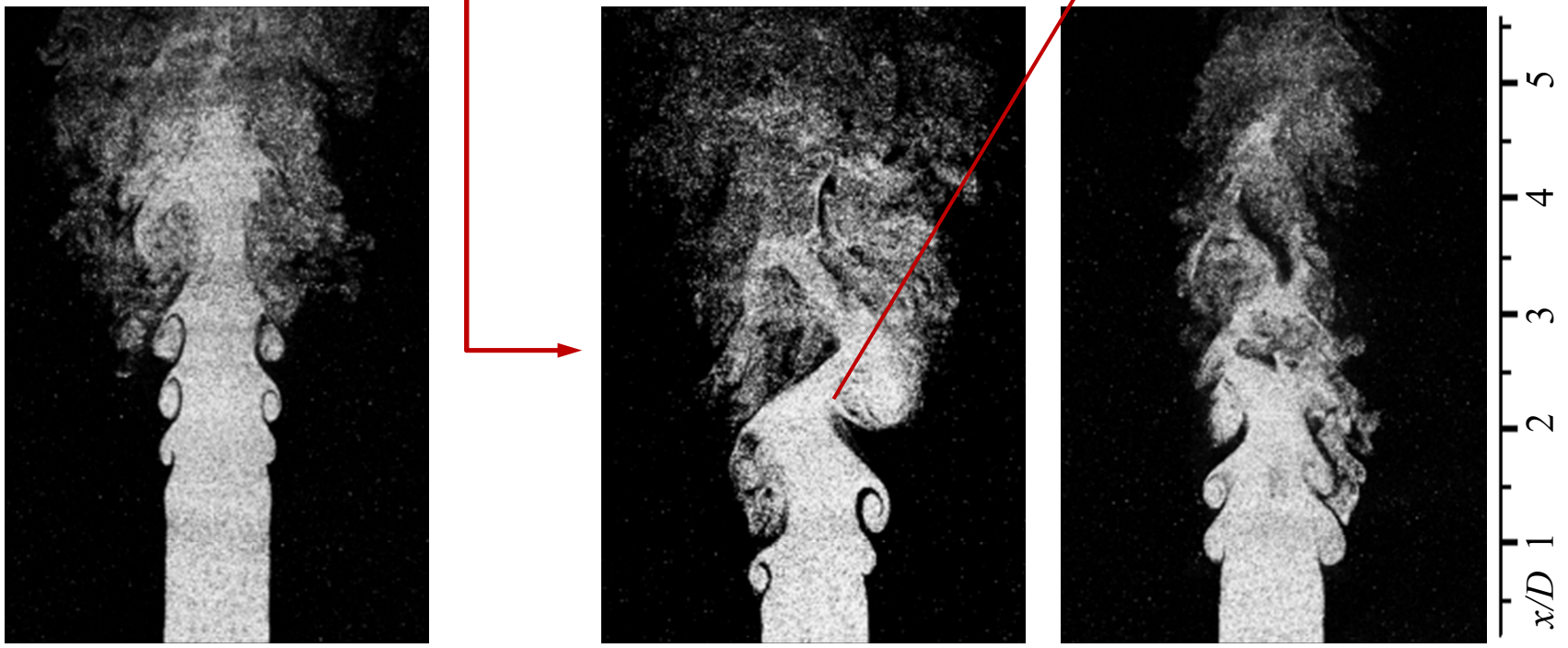

Natural jet

$N = 1$

Flow structure for $N = 1$

Two typical PIV snapshots of instantaneous velocity vectors at $x/D = 2.0$ (C_m=1.4%, $f_e/f_0 = 1$).

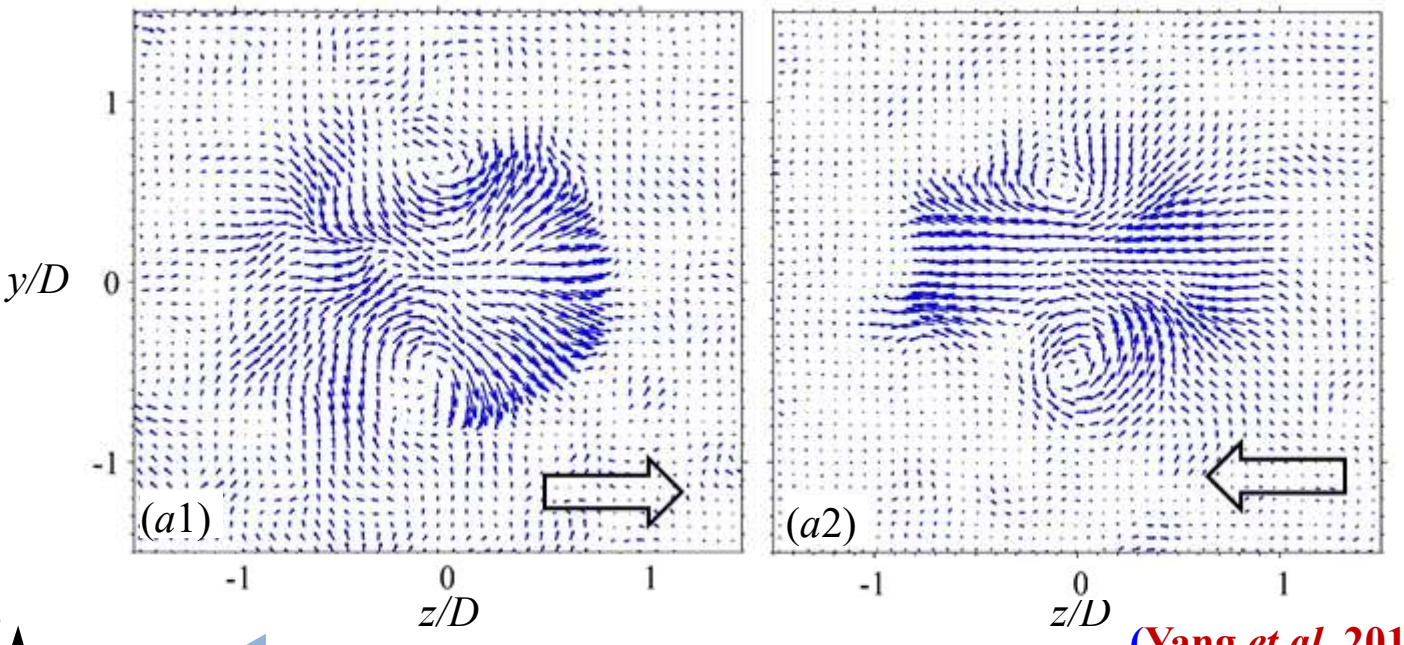

(Yang *et al.* 2016, RSPA)

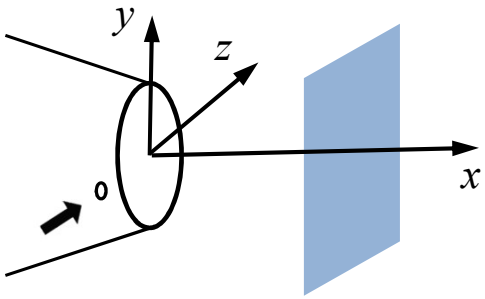

x/D = 2

Flapping of the jet column

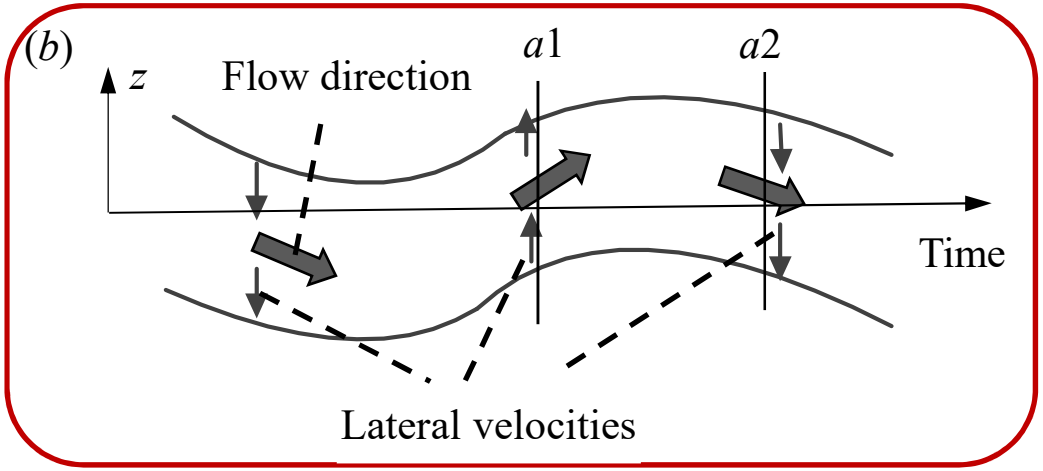

Flow structure for $N = 2$ ($f_e/f_0 = 1$)

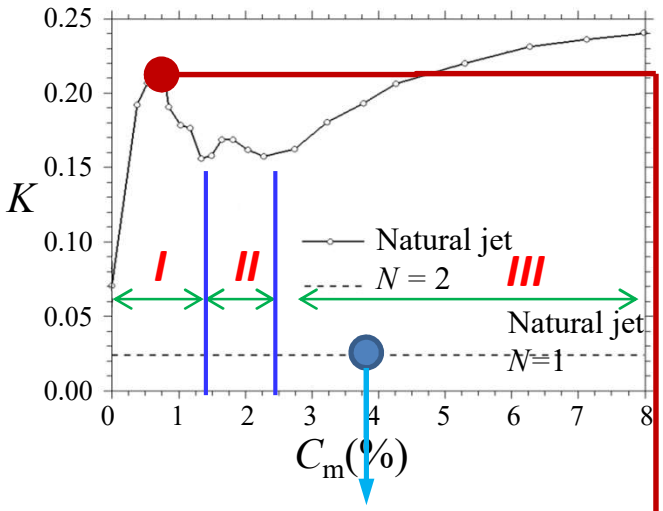

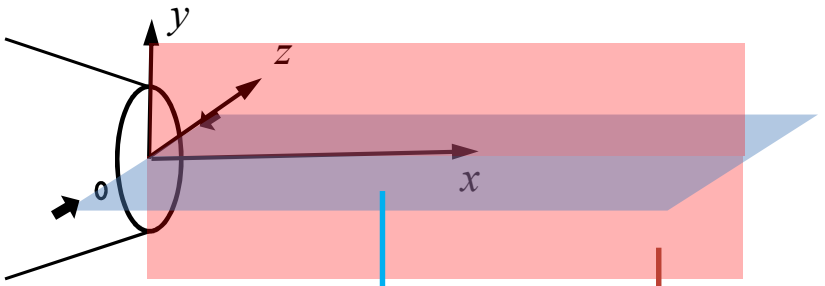

Non-injection plane

Injection plane

Strong entrainment

Rapid spread

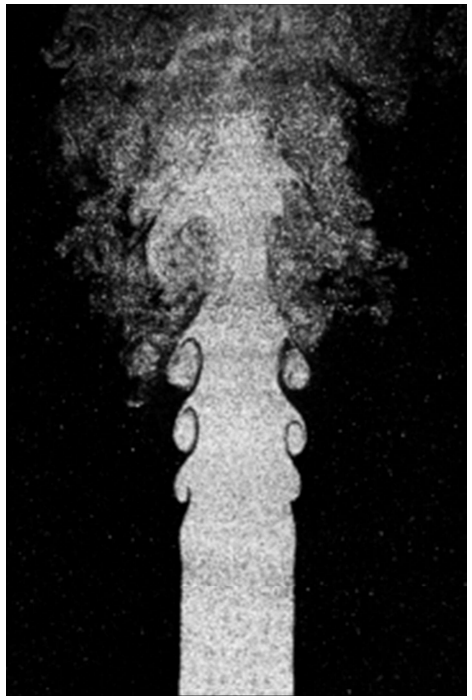

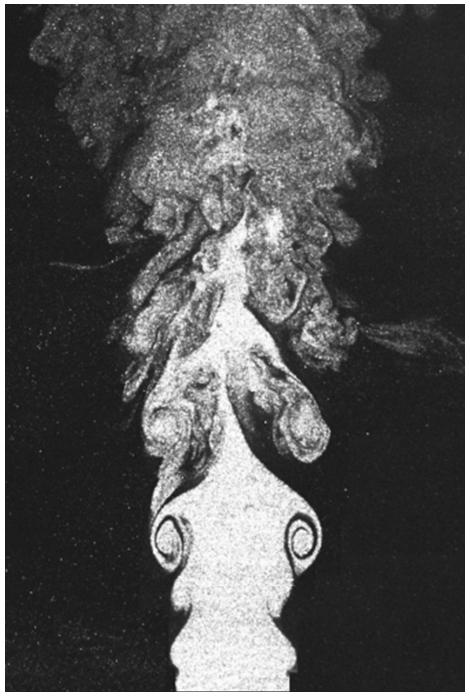

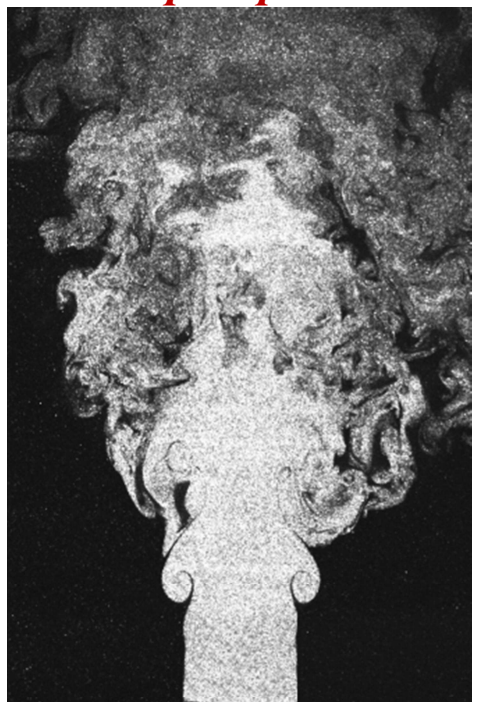

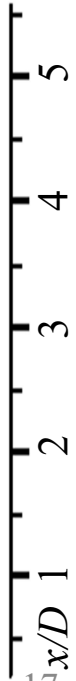

Natural jet

$N = 2$

Cross-sectional flow visualization images

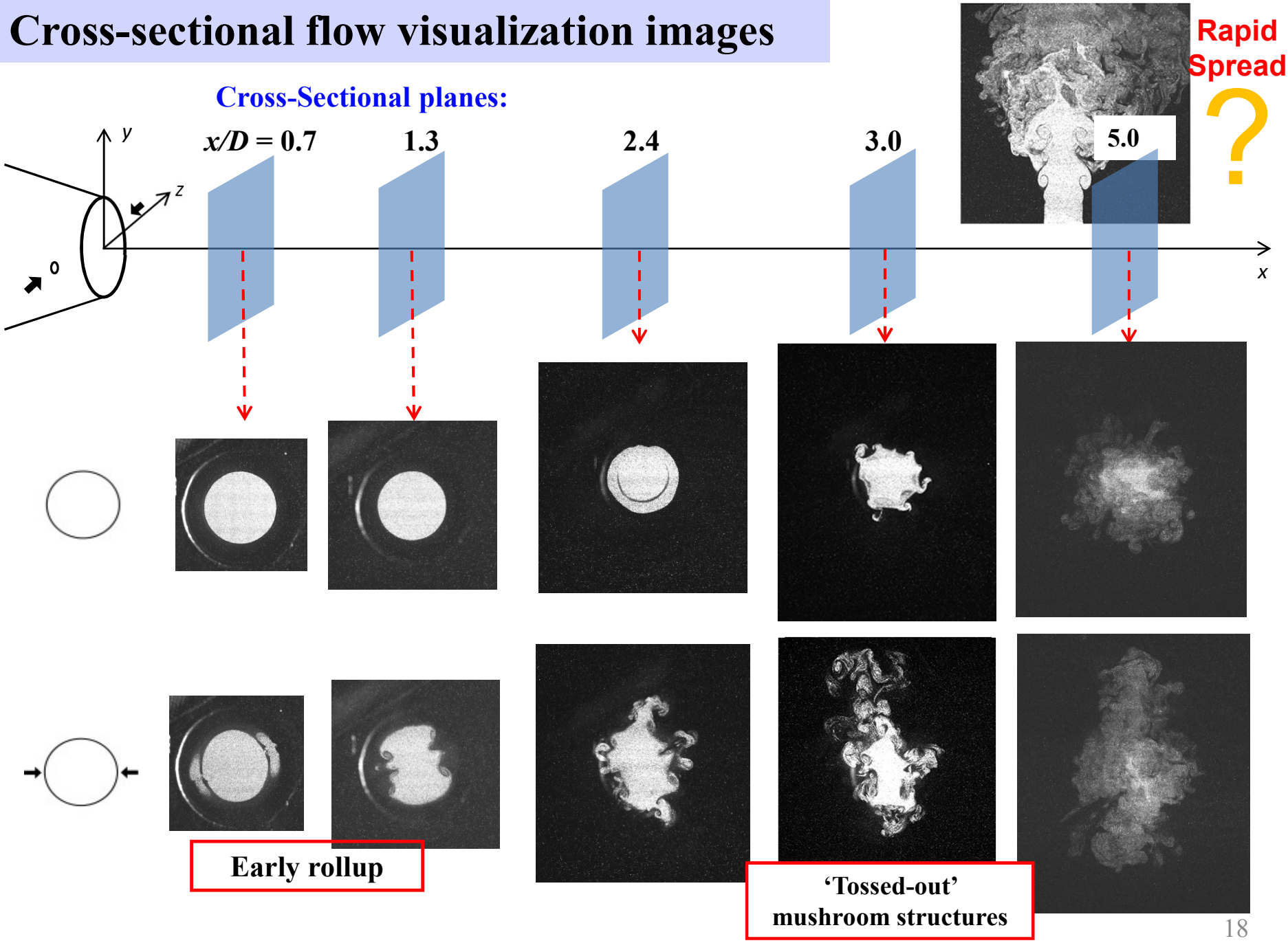

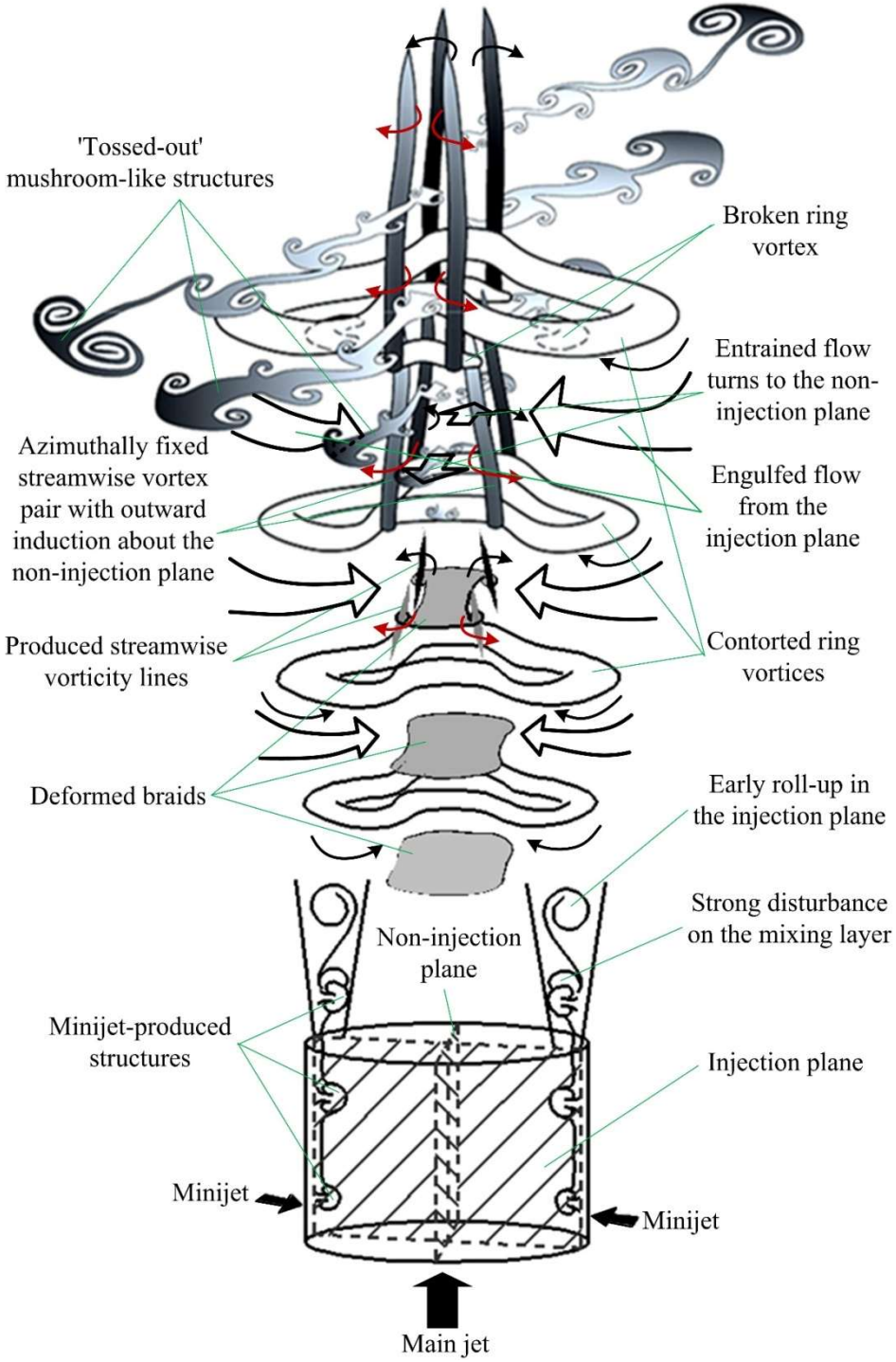

Flow structure model for $N = 2$
Yang & Zhou (2016, JFM)

Past closed-loop control success in the group

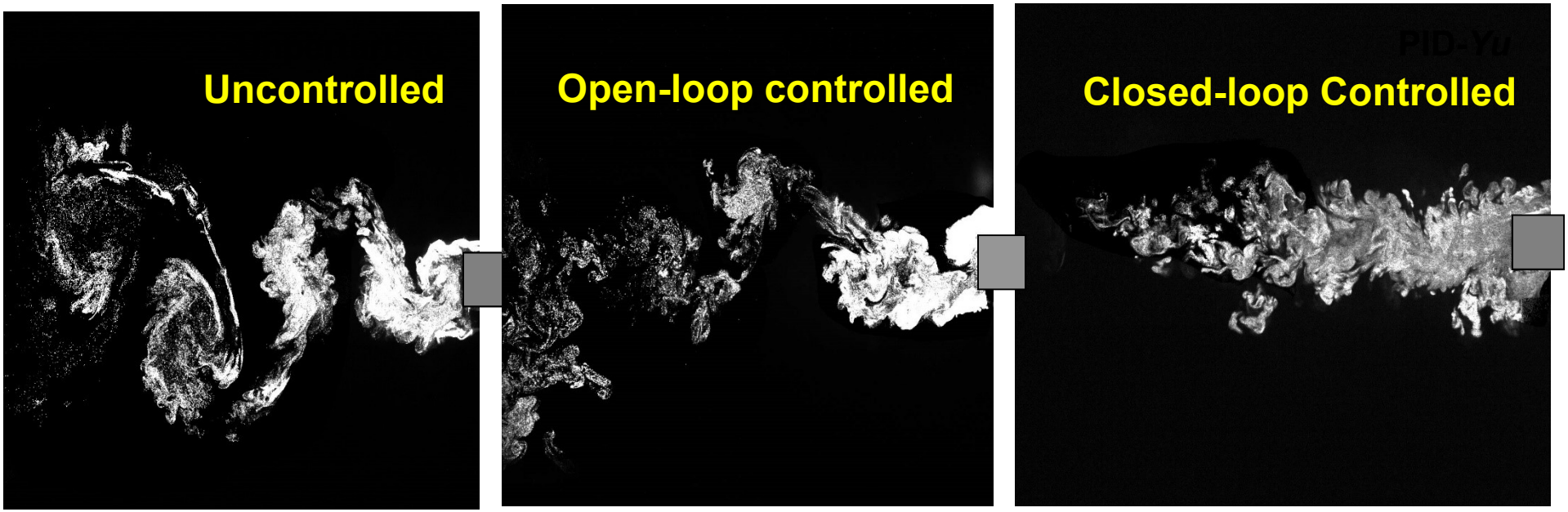

Zhang, Cheng & Zhou (2004 POF)

Closed-loop control: Single-input-single-output system

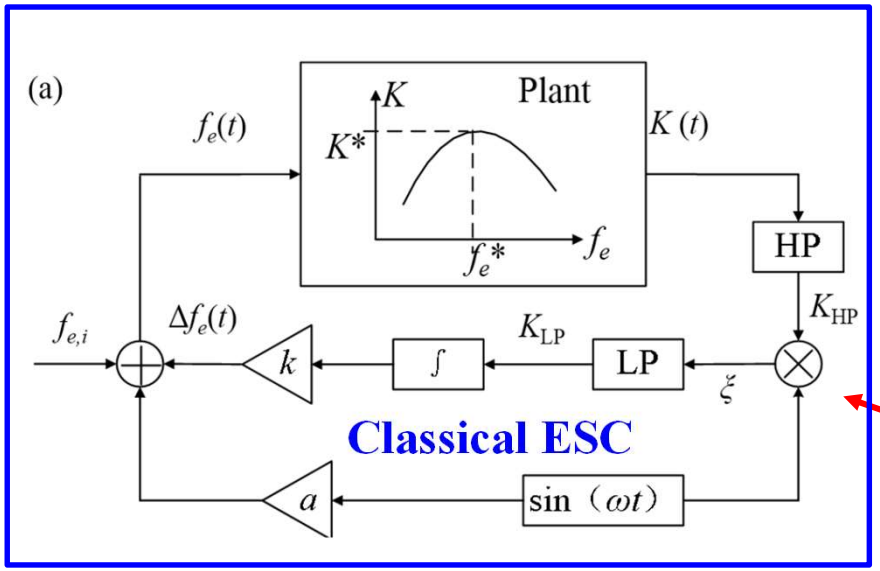

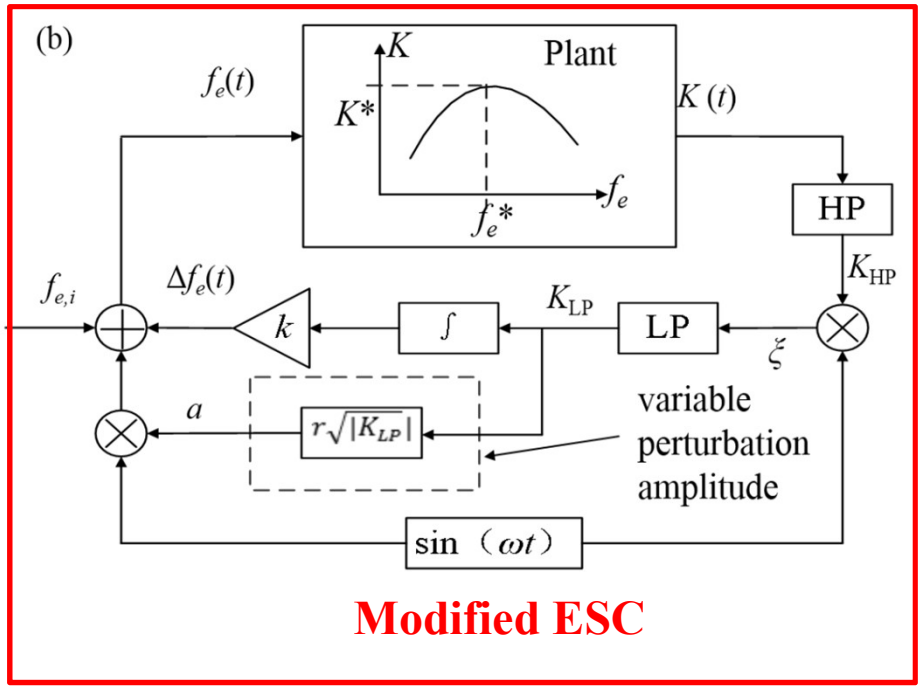

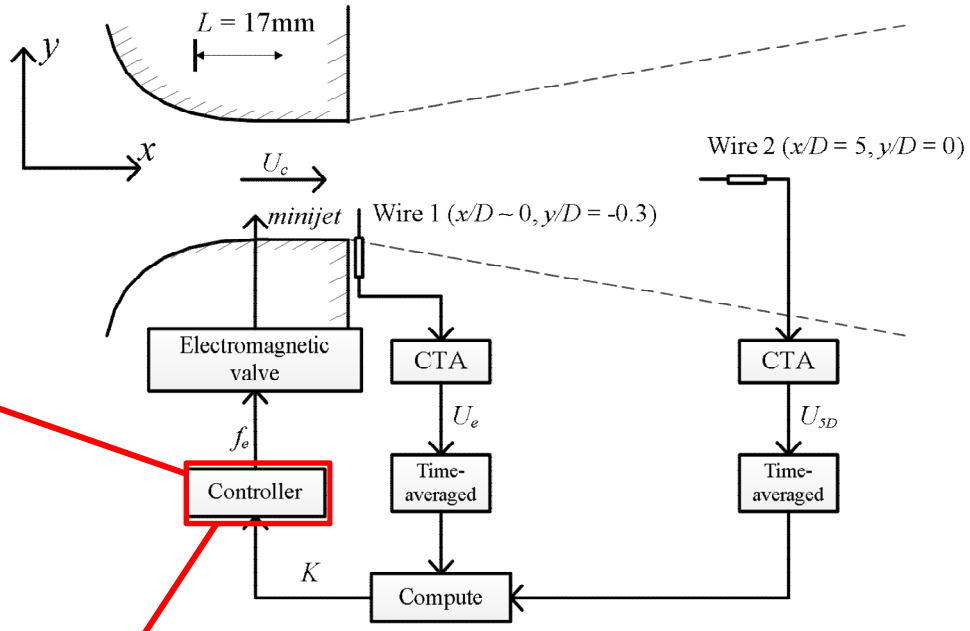

One minijet: C_m = 2.3% (fixed).

Objective

Find $f_{e,optiaml}$ automatically to achieve the maximum *K*.

Wu *et al.* (2016 AIAA J)

Fan *et al.* (2017 AIAA J)

Dual-input-single-output system

A dual-input-single-output (DISO) extremum seeking control (ESC) system is developed with the manipulation of a single minijet. The system manages to seek simultaneously the optimum f_e^* and C_m to achieve the maximum K.

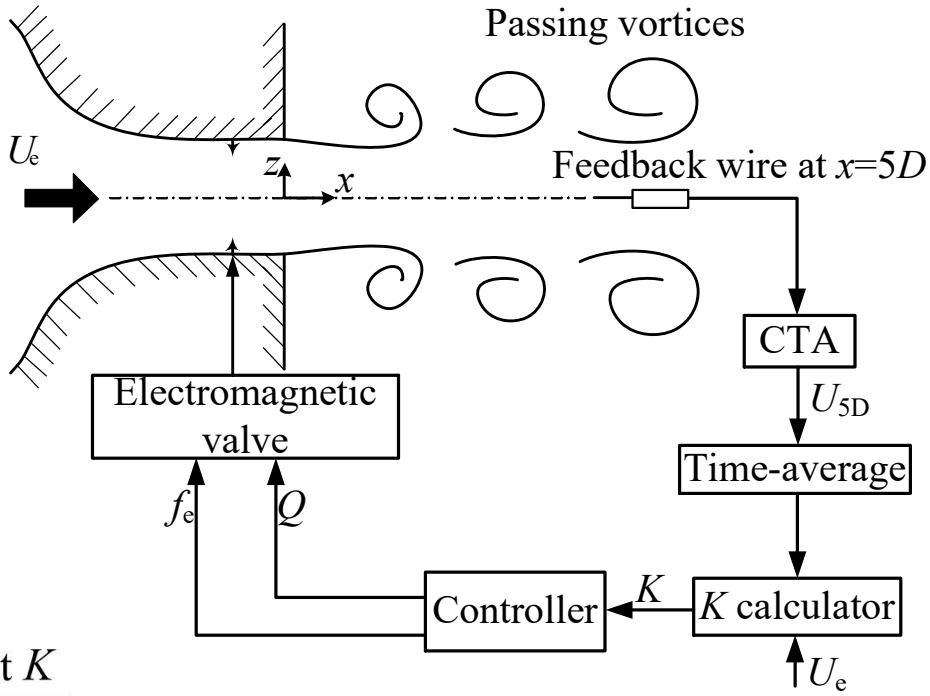

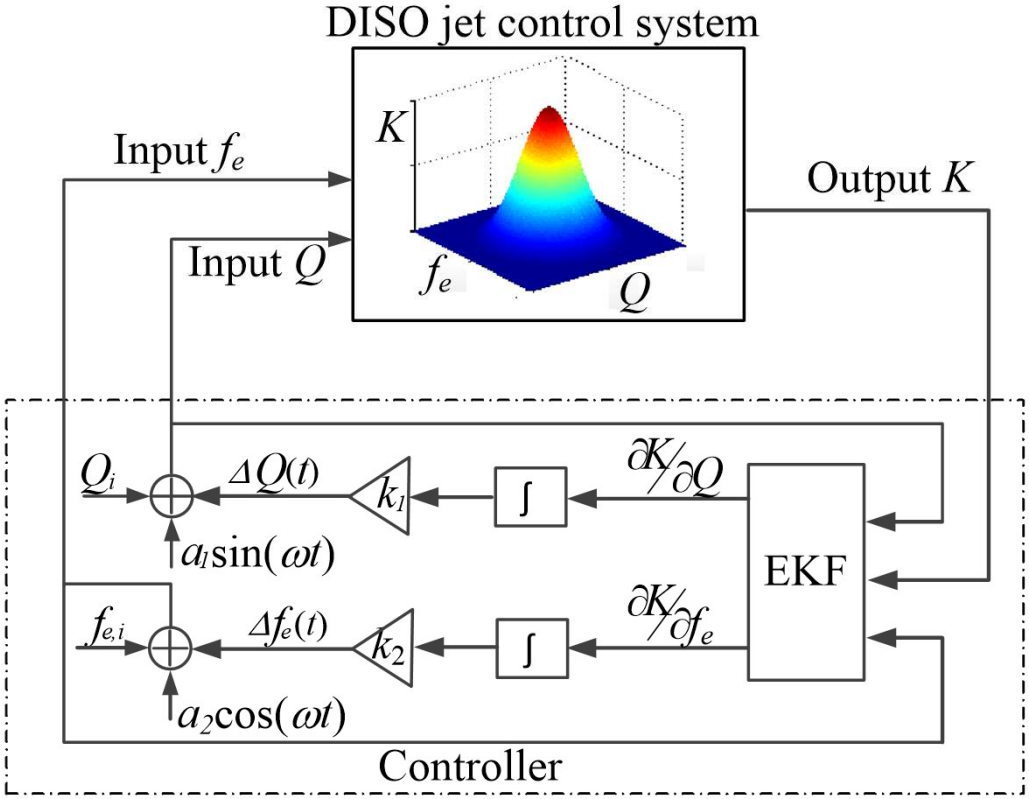

Objective

Find the optimum f_e and C_m automatically to achieve the maximum K.

Responses of the DISO control system *at* $Re_D = 8000$

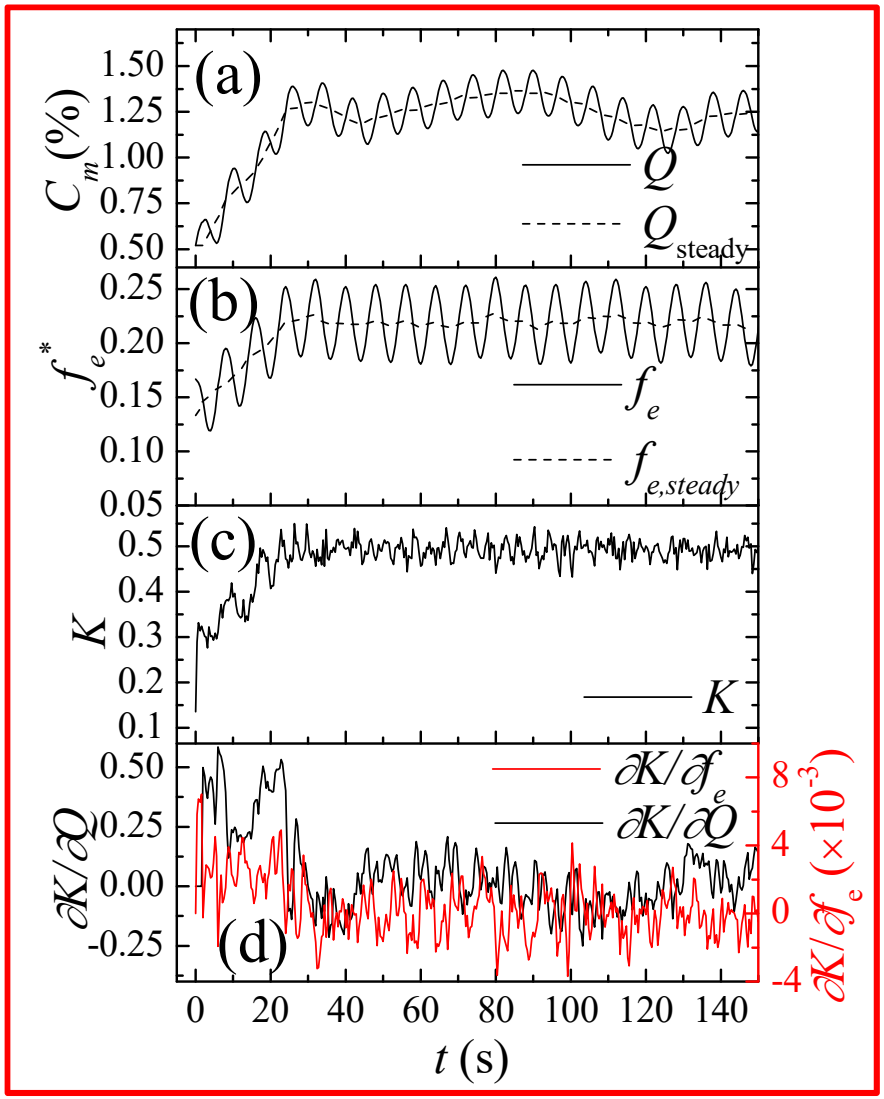

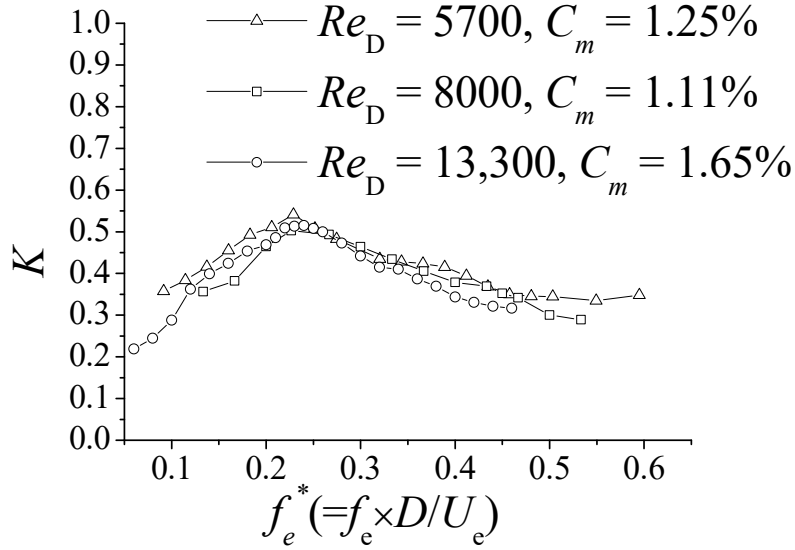

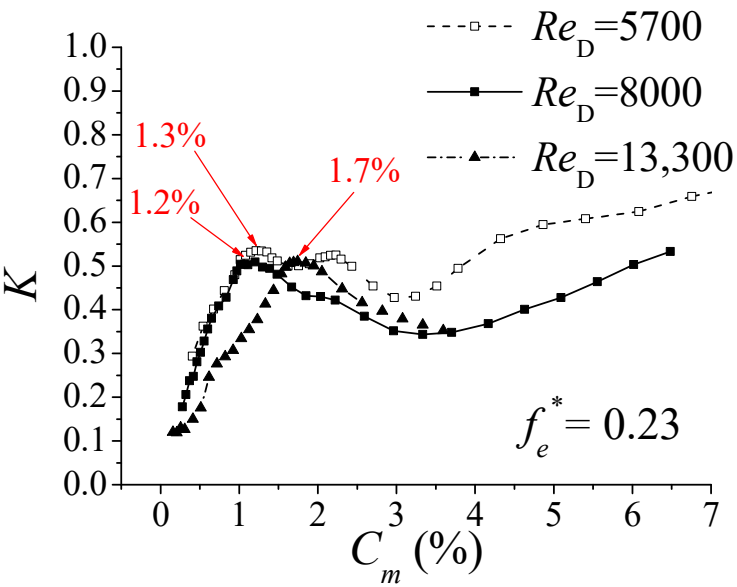

Open-loop control results

Artificial intelligence control

Controller

The control optimization searches for a control law of form

$$\boldsymbol{b} = \boldsymbol{H}\{\boldsymbol{B}(\boldsymbol{s}, \boldsymbol{h}, \boldsymbol{k})\}$$

which minimizes the cost function:

$$\boldsymbol{J = 1 - K}$$

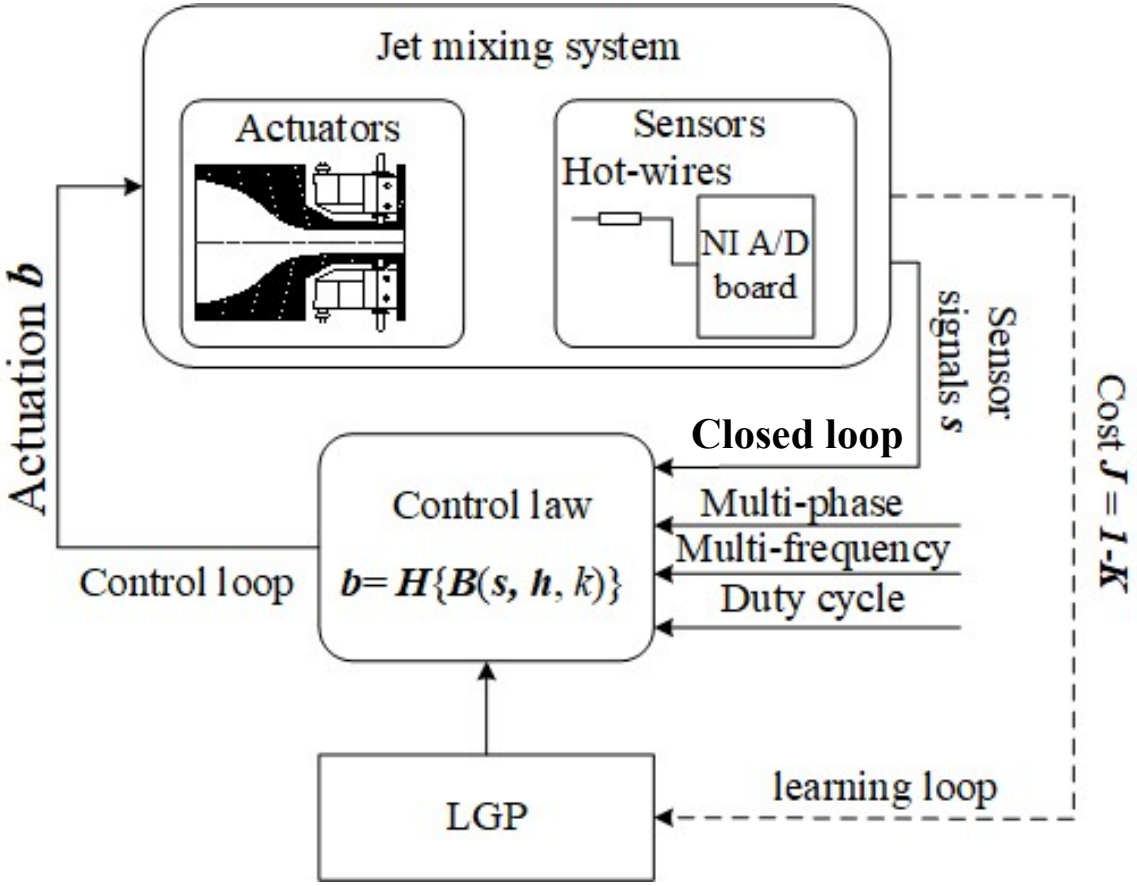

$\boldsymbol{H}$: the Heaviside function.

$\boldsymbol{b} = [b_1, b_2, ..., b_6]^{\dagger}$: actuation commands for the six actuators;

$\boldsymbol{s}$: hot-wire signals measured at $x/D = 0$ and 5;

$\boldsymbol{h} = [h_1, h_2 \ldots, h_{10}]^{\dagger}$: $h_i = \sin(\omega_e t - \phi_i)$, $i = 1, 2, \ldots, 6$, where t is time, ω_e is the excitation frequency, and ϕ_i is a phase, h_7, ... and h_{10} are given by the cosine and sine components of $0.5\omega_e$ *and* $0.25\omega_e$.

$\boldsymbol{k} = [k_1, k_2 \ldots, k_6]^{\dagger}$: k_i is a constant associated with duty cycle α_i.

Linear genetic programming (LGP) — Algorithm

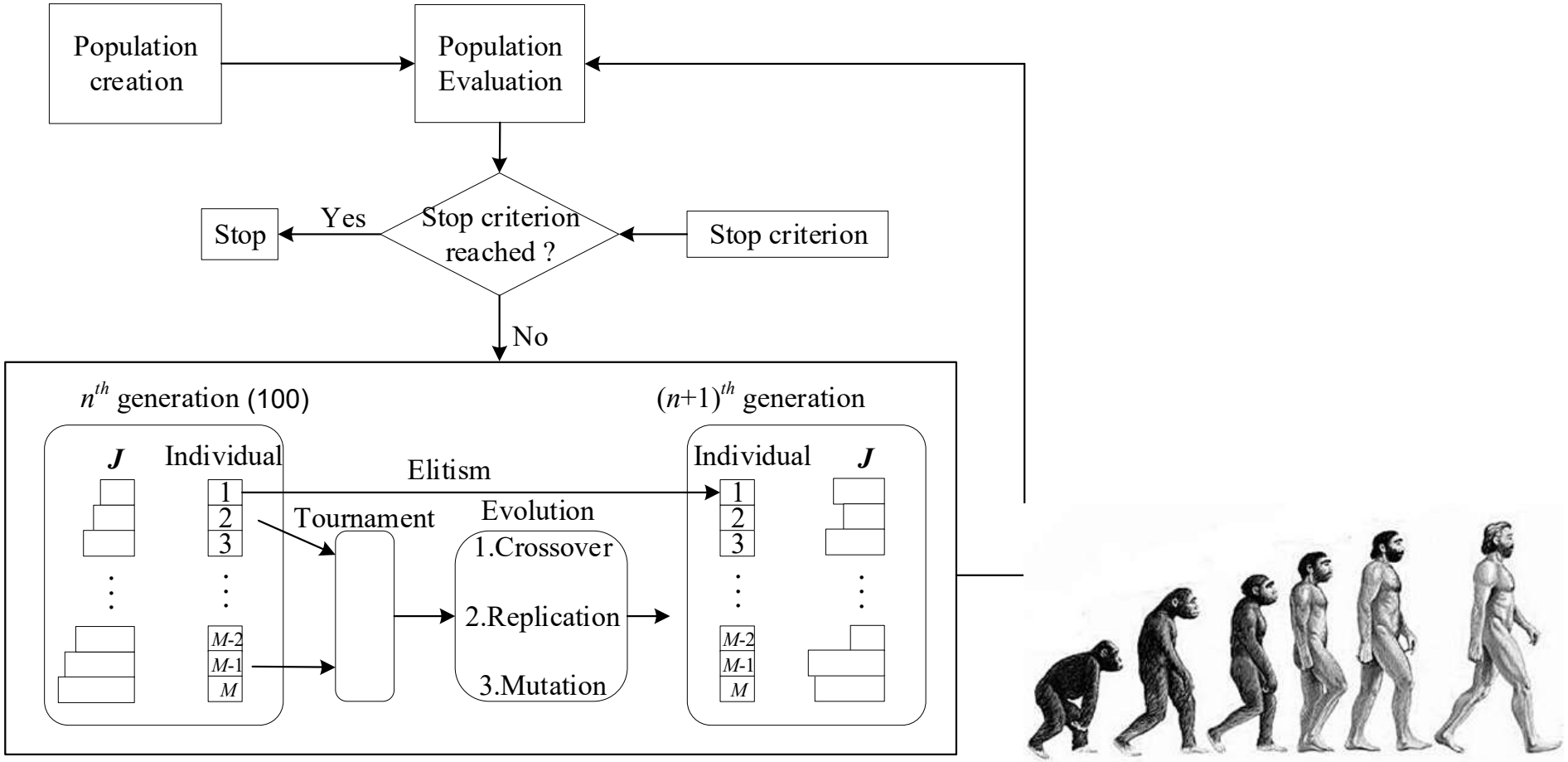

The first generation of LGP, $n = 1$, contains $M = 100$ random control laws, also called ***individuals***. Each individual is tested for 5 seconds in the experiment to yield the measured cost J_i^1 , where superscript 'i' represents the individual testing number. Subsequent generations are generated from the previous ones with genetic operations (***elitism, crossover, mutation and replication***) and tested analogously. After the *in situ* performance measurements, the individuals are re-numbered in order of performance, $J_1^n \leq J_2^n \leq \ldots \leq J_M^n$, where the superscript 'n' represents the generation number.

Presentation of results

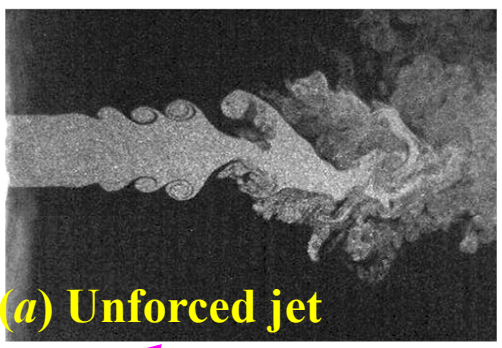

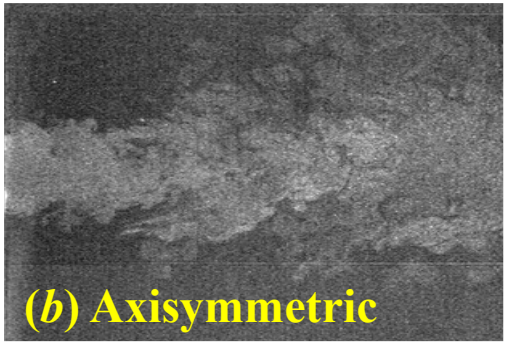

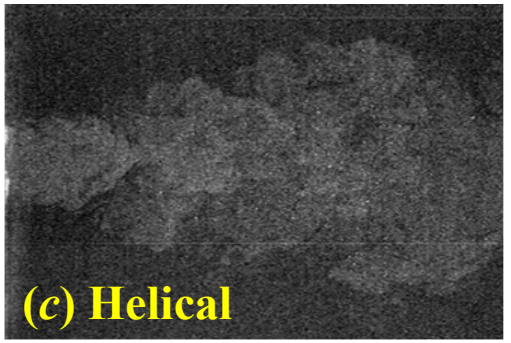

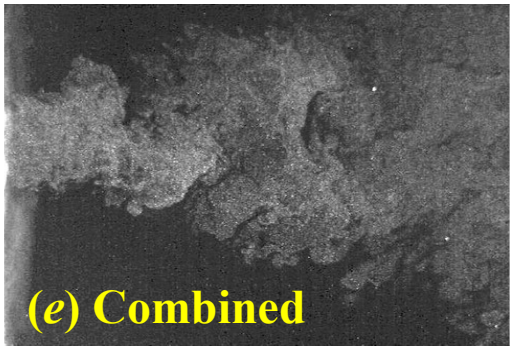

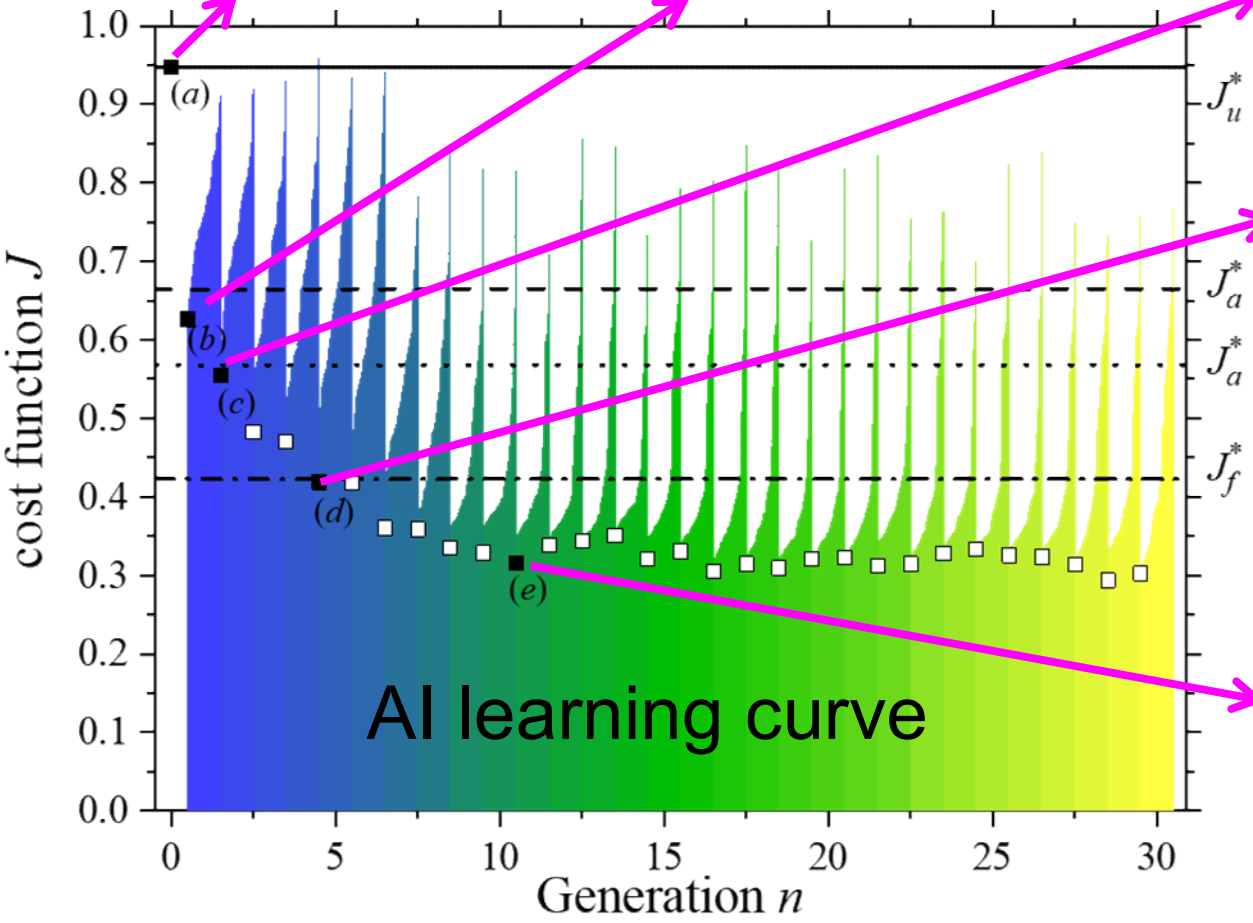

Injecting minijets for generations n = 1, 2, 5 and 11, $\phi = \pi/3, 2\pi/3, \pi, \ldots, 2\pi$ corresponding to consecutive times $t = \phi T/2\pi$ in one period. Each of the six sectors of the circles represents one minijet.

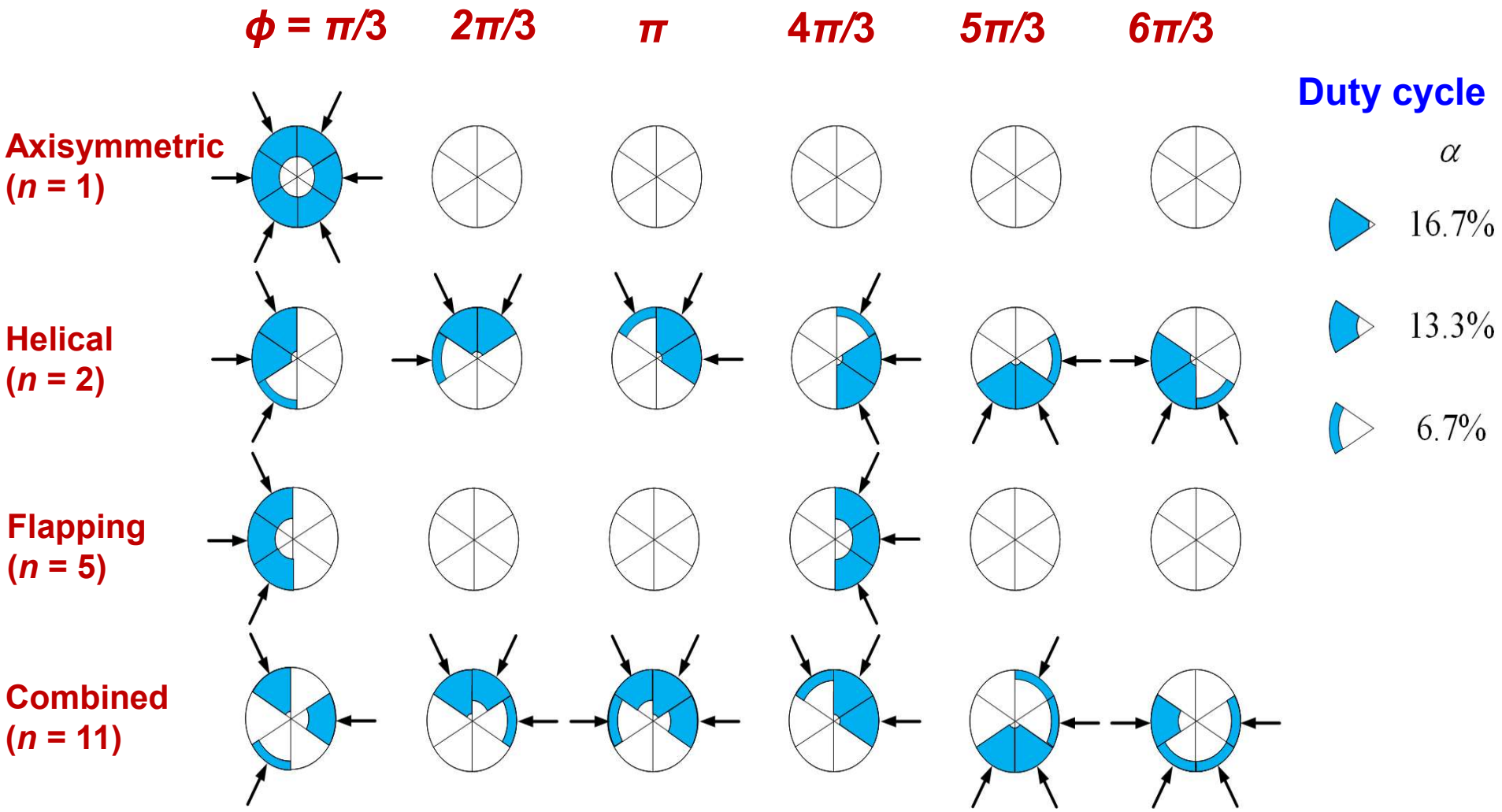

AI-produced flow structures

Axisymmetric forcing $n = 1$

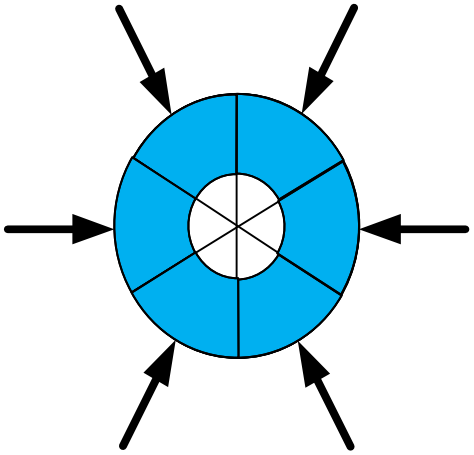

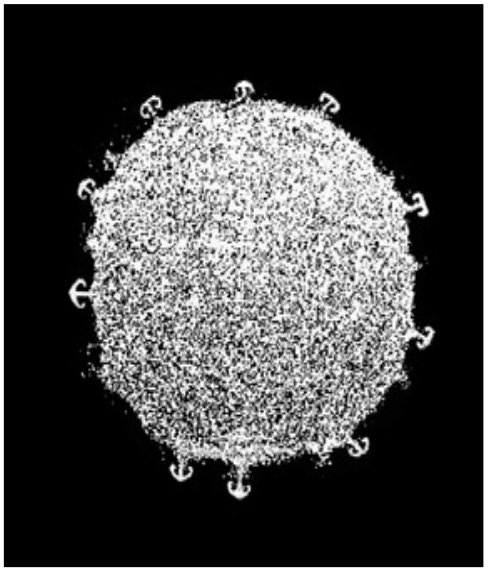

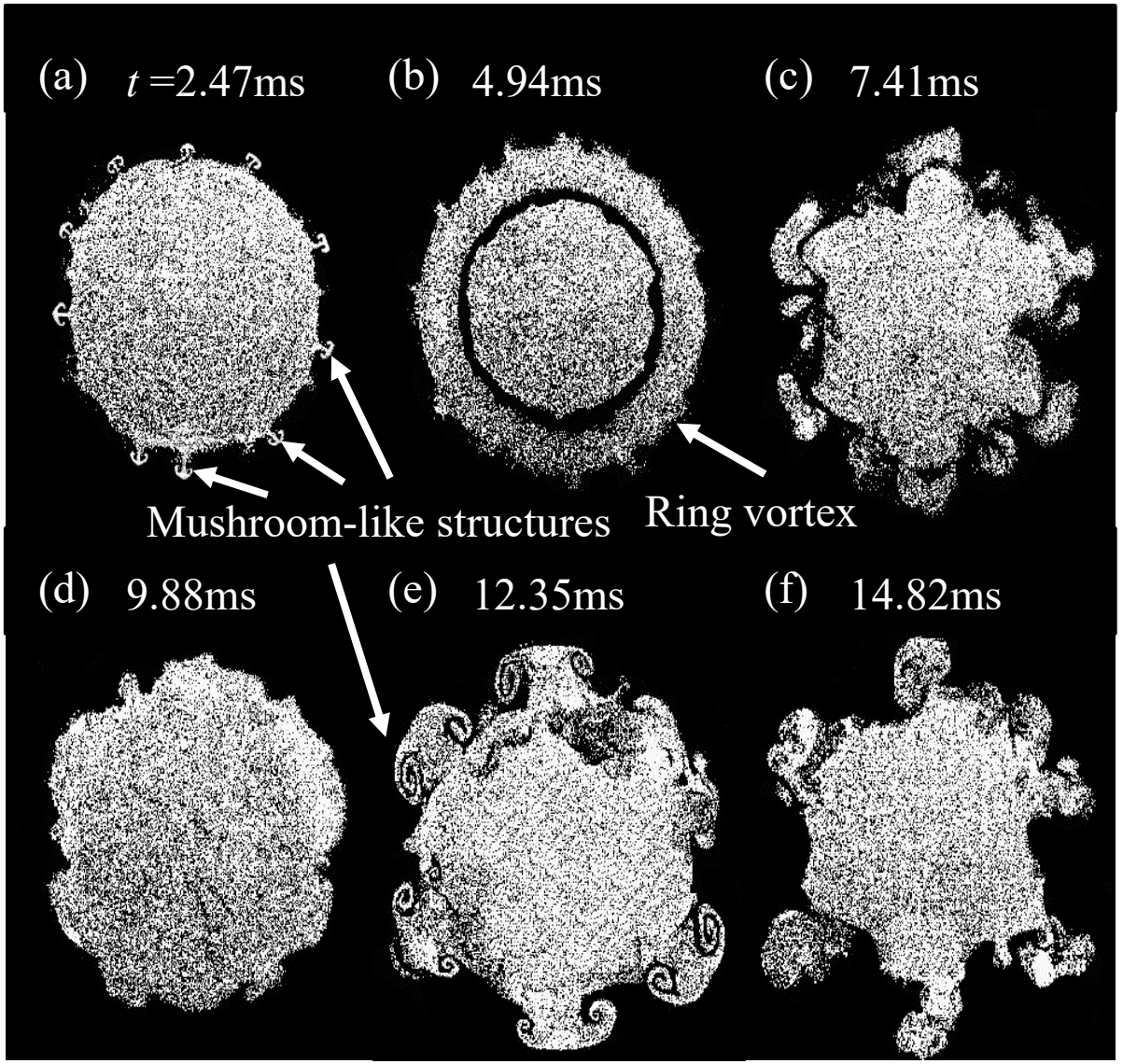

Photographs of typical flow structures from flow visualization under symmetric minijet forcing in a continuous time sequence at $x/D = 0.25$. Flow is outward from the paper.

Helical forcing $n = 2$

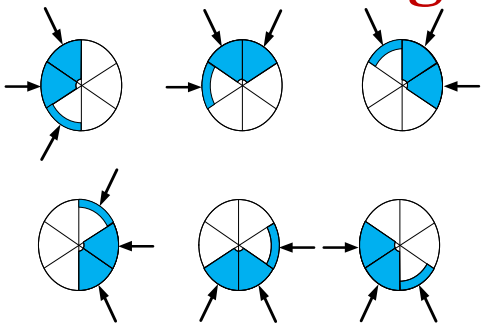

The (y, z) plane

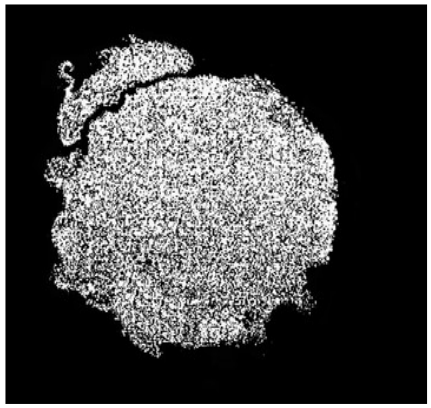

The (x,y) plane

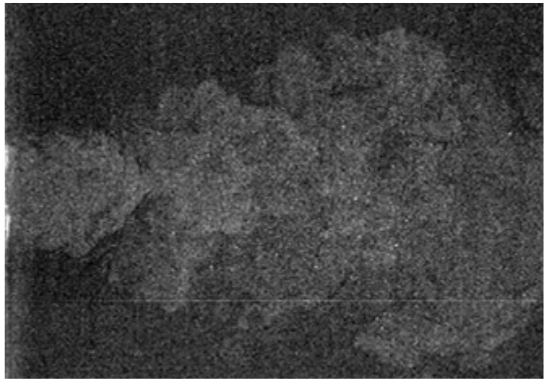

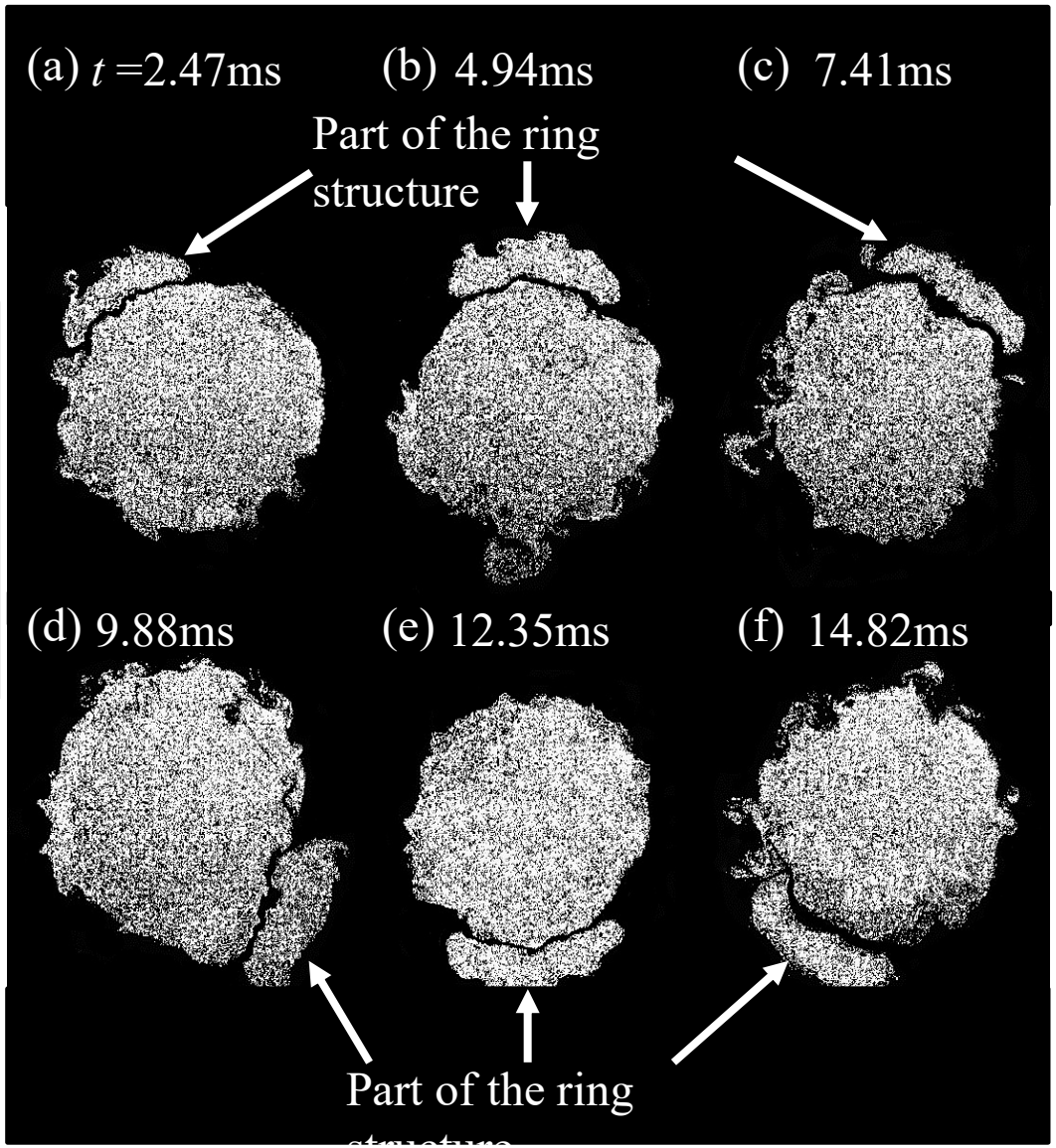

Photographs of typical flow structures from flow visualization under rotating forcing in a continuous time sequence at $x/D = 0.25$. Flow is outward from the paper.

Flapping forcing $n = 5$

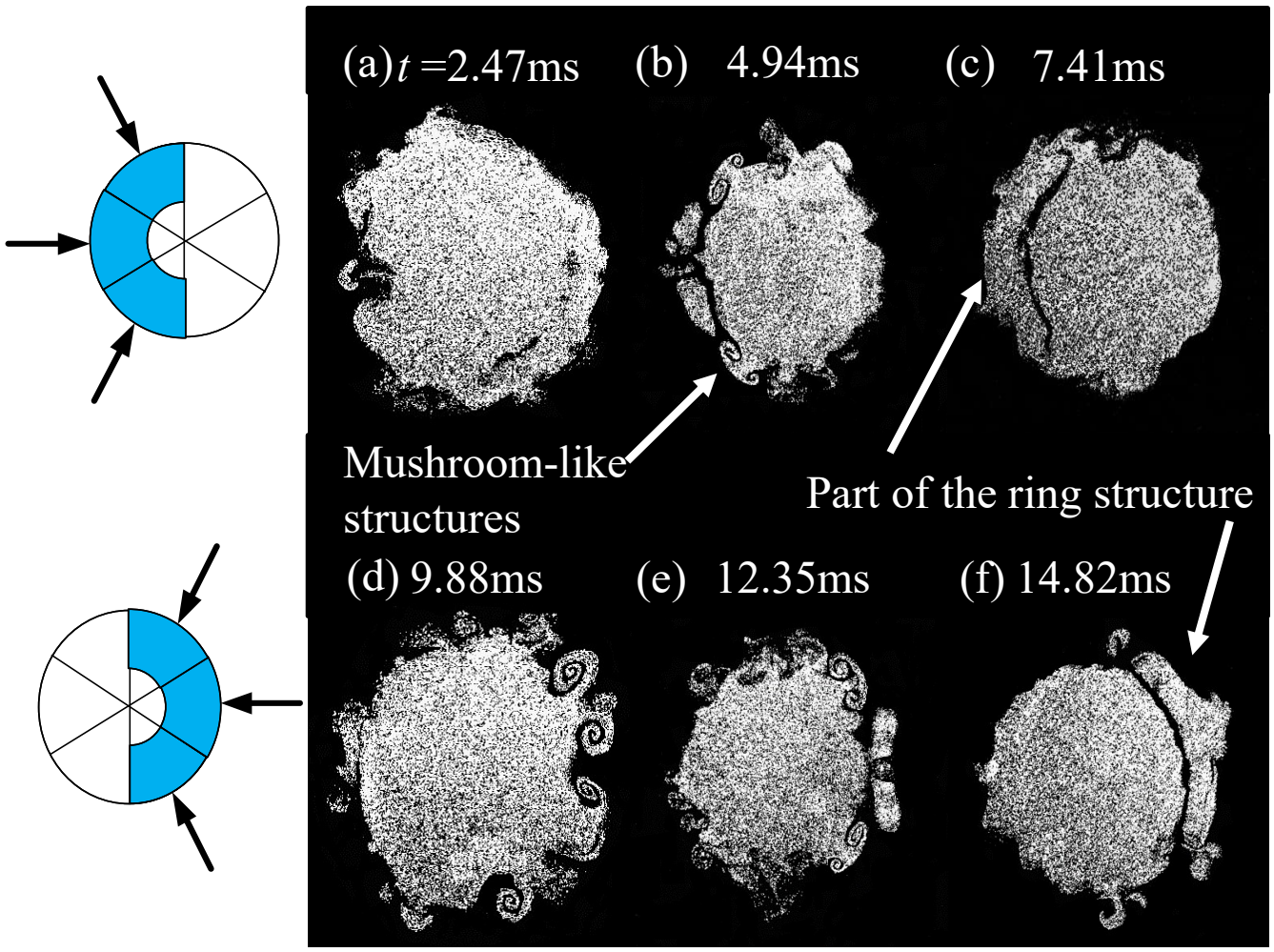

The (y, z) plane

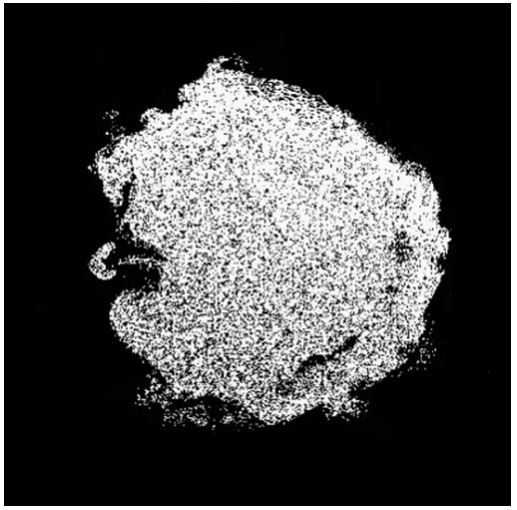

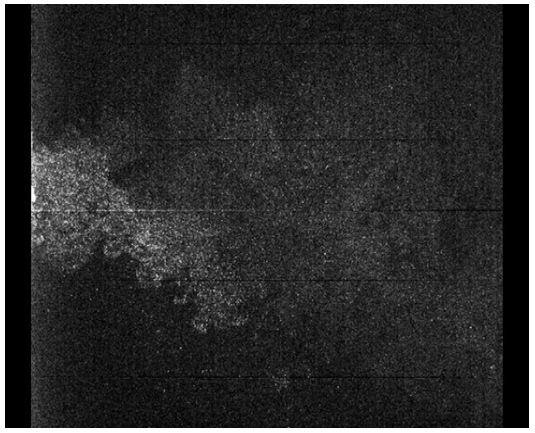

The (x, y) plane

Photographs of typical flow structures from flow visualization under flapping forcing in a continuous time sequence at $x/D = 0.25$. Flow is outward from the paper.

Combined forcing $n = 11$

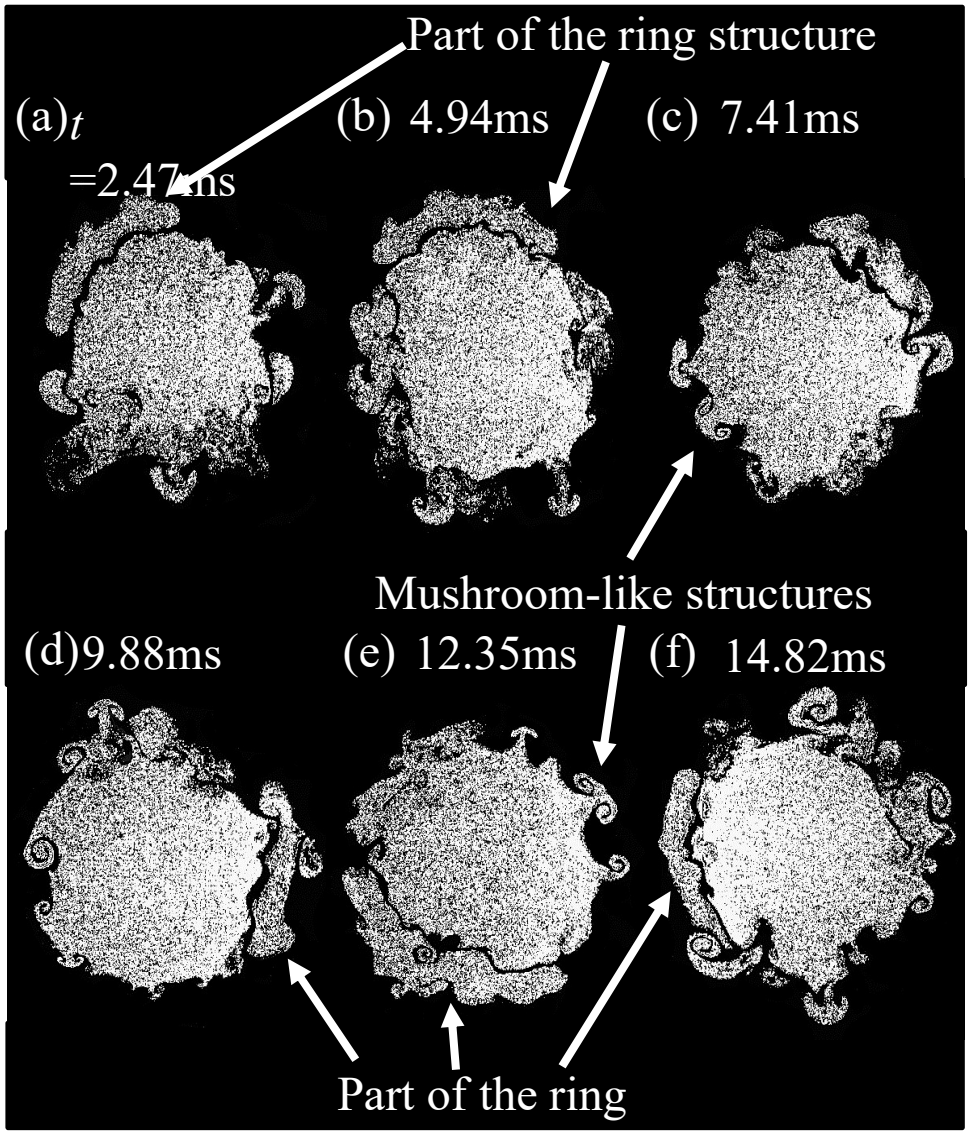

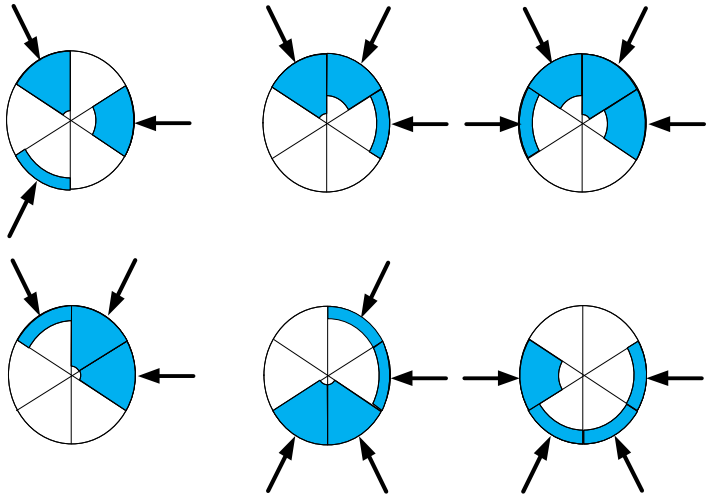

The (y, z) plane

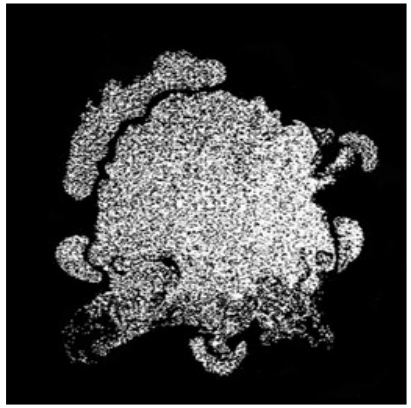

The (x, y) plane

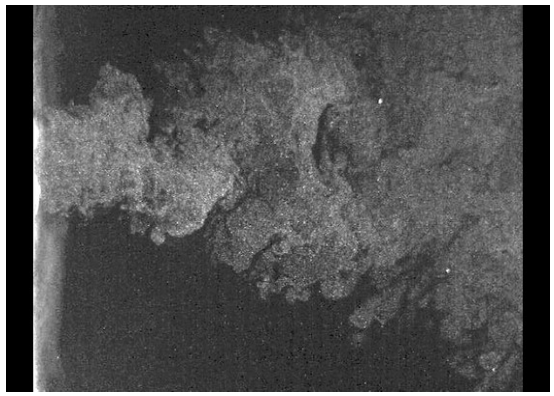

Photographs of typical flow structures from flow visualization under flapping and rotating forcing in a continuous time sequence at $x/D = 0.25$. Flow is outward from the paper.

EPOD reconstructed velocity iso-surface

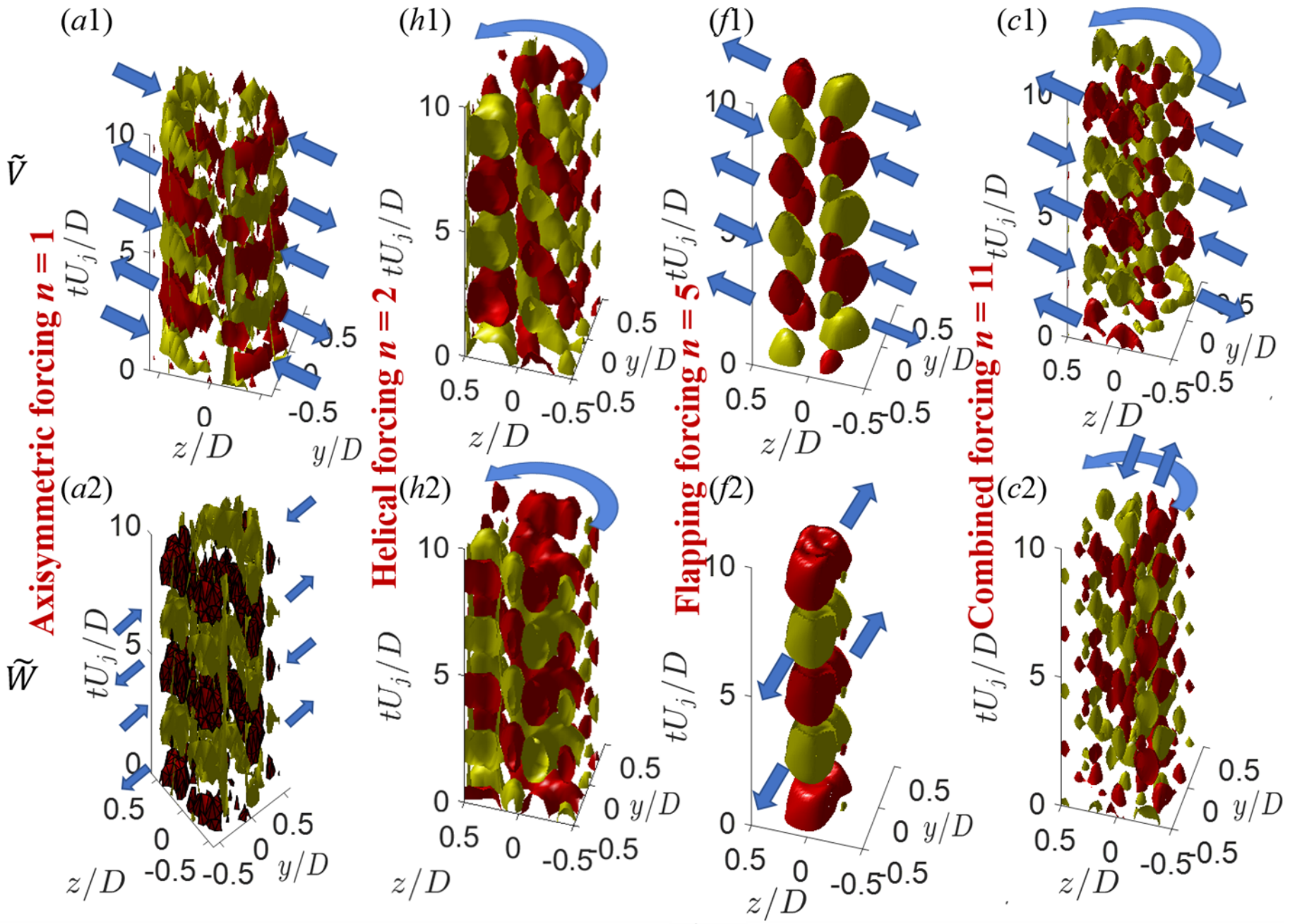

Conclusions

1 AI control has identified three classical forcings in its learning process and is converged to a sophisticated spatio-temporal actuation, which vastly outperforms others.

2 The AI-learned globally optimal solution is reproducible with other initial inputs, and does not depend on the parameters of the genetic programming.

3 The proximity maps unveil that all data points or control laws tend to occur in three regions, characterized by axisymmetric, helical and flapping forcings, respectively. The globally optimized control law occurs in the region of 'mutated' helical forcing.

4 AI produces a sophisticated flow structure, never reported before, and characterized by (1) swirling, (2) changing axis of swirling, (3) changing speed of swirling, (4) 3D oscillation, and (5) generating mushroom-like structures.